

X-ray spectroscopy of Cu impurities on NSTX and comparison with Z-pinch plasmas^{a)}

A. S. Safronova,^{1,b)} N. D. Quart,¹ J. K. Lepson,² P. Beiersdorfer,³ B. Stratton,⁴ M. Bitter,⁴ V. L. Kantsyrev,¹ P. G. Cox,¹ V. Shlyaptseva,¹ and K. M. Williamson¹

¹University of Nevada, Reno, Nevada 89557, USA

²Space Sciences Laboratory, Berkeley, California 94720, USA

³Lawrence Livermore National Laboratory, Livermore, California 94550, USA

⁴Princeton Plasma Physics Laboratory, Princeton, New Jersey 08543, USA

(Presented 19 May 2010; received 16 May 2010; accepted 21 June 2010; published online 5 October 2010)

X-ray spectroscopy of mid-Z metal impurities is important in the study of tokamak plasmas and may reveal potential problems if their contribution to the radiated power becomes substantial. The analysis of the data from a high-resolution x-ray and extreme ultraviolet grating spectrometer, XEUS, installed on NSTX, was performed focused on a detailed study of x-ray spectra in the range 7–18 Å. These spectra include not only commonly seen iron spectra but also copper spectra not yet employed as an NSTX plasma impurity diagnostic. In particular, the L-shell Cu spectra were modeled and predictions were made for identifying contributions from various Cu ions in different spectral bands. Also, similar spectra, but from much denser Cu plasmas produced on the UNR Z-pinch facility and collected using the convex-crystal spectrometer, were analyzed and compared with NSTX results. © 2010 American Institute of Physics. [doi:10.1063/1.3478673]

I. INTRODUCTION

The presence of metallic ions (such as, for example, Fe, Ni, or Cu) in tokamak plasmas usually indicates that the hot plasma is ablating or melting specific machine components, influencing the plasma conditions of a magnetic fusion device. Spectroscopy is an appropriate tool to detect the impurities in such plasmas and their concentration.¹ It provides valuable information on which components were affected and how much. In particular, x-ray spectroscopy of mid-Z impurities is useful to study core and near-core plasma regions in tokamaks and may reveal potential problems if the radiated power is found to be significant. Substantial progress in identifying mid-Z impurities in NSTX plasma through spectroscopy was made with the installation and utilization of two high-resolution grating spectrometers: the x-ray and extreme ultraviolet spectrometer² (XEUS) and the long wavelength extreme ultraviolet spectrometers LoWEUS.³ Extreme ultraviolet (EUV) and x-ray spectra from metal impurities on NSTX recorded with XEUS and LoWEUS were recently presented in Ref. 4. Such spectra can potentially provide important information about the plasma and metal impurities and their concentration. In particular, in this work we study in detail x-ray spectra recorded by XEUS on NSTX in a spectral range from 7 to 18 Å. These spectra include not only commonly seen iron spectra but also copper spectra. Such copper spectra have not been yet employed in NSTX as a plasma impurity diagnostic and their

detailed study represents the main focus of this paper. Both L-shell Cu and Fe spectra were analyzed in detail. Similar Cu x-ray spectra, but from much denser plasmas produced on Zebra Z-pinch facility at UNR (see, for example, Ref. 5), were analyzed and compared with the NSTX measurements.

II. THEORETICAL DIAGNOSTIC TOOL: IDENTIFICATION AND MODELING OF PROMINENT L-SHELL SPECTRAL FEATURES

Nonlocal thermodynamic equilibrium collisional-radiative atomic kinetic models of Cu, Fe, and Ni have been employed in this work. These models include all the ground states from the bare ion to the neutral atom as well as atomic structure details for some of the ions. In particular, the Cu model includes structure details of the ions from H-like to Al-like for a total of 4939 levels and is utilized here to model the L-shell Cu spectra from the Z-pinch and NSTX plasmas. In addition, Fe and Ni models with a similar number of levels included are employed in this work in the analysis of the NSTX L-shell spectra. The energy level structure and complete radiative and collisional coupling were calculated by the flexible atomic code.⁶ These models were employed before to describe the radiation from Z-pinch and laser-produced plasmas. For example, the Cu model was successfully used to study the L- and K-shell radiations from X-pinch⁷ and cylindrical⁸ and planar wire arrays⁵ on the 1MA Zebra facility at UNR. The synthetic spectra calculated using these models are presented in Figs. 1–3. For example, the L-shell Cu spectrum covers the spectral region from 7 to 14 Å. The most intense L-shell Cu lines are the Ne-like resonance lines due to 3-2 transitions labeled 3A-3G, which occupy the spectral region from 10.58 to 12.85 Å. The most

^{a)} Contributed paper, published as part of the Proceedings of the 18th Topical Conference on High-Temperature Plasma Diagnostics, Wildwood, New Jersey, May 2010.

^{b)} Author to whom correspondence should be addressed. Electronic mail: alla@unr.edu.

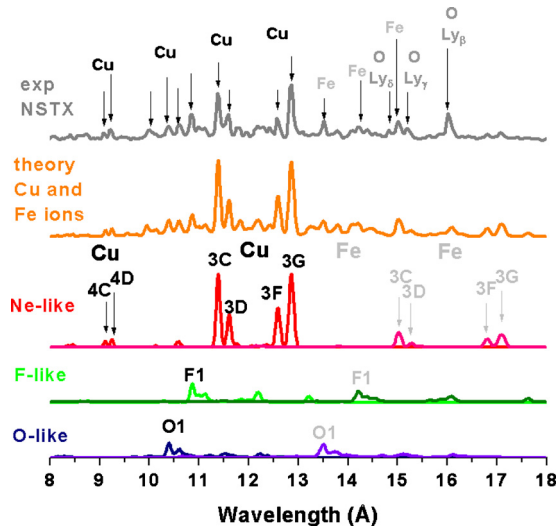


FIG. 1. (Color online) Experimental spectrum from NSTX with identified spectral features and corresponding theoretical synthetic spectra from L-shell Cu and Fe ions.

intense lines are line 3C ($1s^22s^22p^53d^1P_1-1s^22s^22p^6^1S_0$) at 11.390 Å, 3D ($1s^22s^22p^53d^3D_1-1s^22s^22p^6^1S_0$) at 11.608 Å, 3F ($1s^22s^22p^53s^1P_1-1s^22s^22p^6^1S_0$) at 12.591 Å, and 3G ($1s^22s^22p^53s^3P_1-1s^22s^22p^6^1S_0$) at 12.849 Å. The intensities of the 3F and 3G lines depend on radiative cascades from highly excited states in the Ne-like ion and as the electron density increases, these radiative cascades begin to be influenced by collisional processes. As a result, the relative intensities of the 3G and 3F lines are sensitive to the electron density n_e higher than 10^{18} cm $^{-3}$. The most intense line 3C has the highest radiative decay and is optically thick for most Z-pinch experiments considered here. For diagnostics it is also convenient to use the less intense Ne-like lines from the higher Rydberg states, i.e., $n=4, 5$, and 6, which are expected to be less effected by opacity than the 3C and 3D lines. These lines include lines 4C at 9.115 Å ($1s^22s^22p^54d^1P_1-1s^22s^22p^6^1S_0$) and 4D at 9.245 Å ($1s^22s^22p^54d^3D_1-1s^22s^22p^6^1S_0$).⁵ The appearance of strong spectral features from F-like ions and from even higher ionization stages of

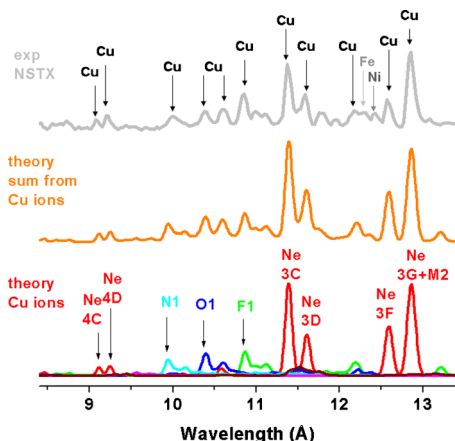


FIG. 2. (Color online) A part of the NSTX experimental spectrum between 8.5 and 13.5 Å featuring L-shell Cu and small contribution from L-shell Fe and Ni and corresponding synthetic L-shell Cu spectra.

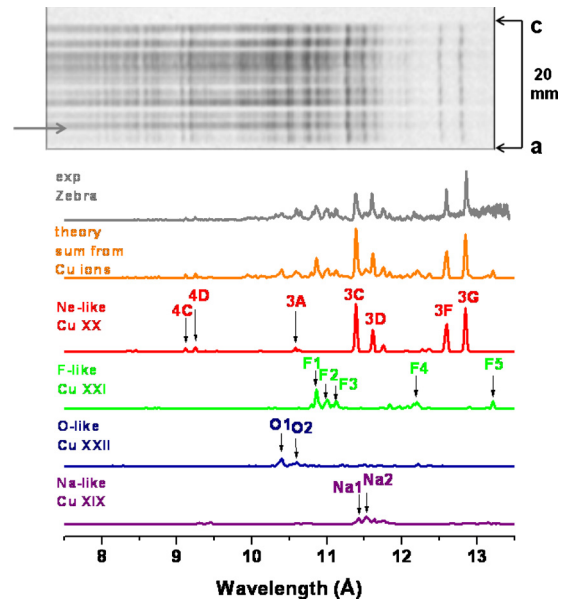


FIG. 3. (Color online) An x-ray image and lineout of the experimental spectrum from the implosion of a Cu planar wire array produced at the 1 MA Zebra generator at UNR and corresponding theoretical synthetic spectra from L-shell Cu ions. At the top, an arrow indicated the position of the lineout between the anode (a) and cathode (c).

O- and N-like ions usually indicates a much higher electron temperature than that associated with the Ne-like lines.

III. ANALYSIS OF NSTX IMPURITY SPECTRA DOMINATED BY L-SHELL Cu EMISSION

The most common seen metal impurity in NSTX experiments is iron, followed by nickel and copper. Iron and nickel come from the stainless steel outer wall and hardware, and copper is found in the rf heating antennae and associated shielding. EUV and x-ray spectra from metal impurities on NSTX recorded with XEUS and LoWEUS were recently presented in Ref. 4. This paper focuses on the analysis of x-ray spectra recorded by XEUS which has an ~ 50 Å field of view that can be positioned to cover a spectral region from 5 to 135 Å. In this work we study in detail x-ray spectra recorded in the spectral range from 7 to 18 Å. These spectra include not only the commonly seen iron spectra but also copper spectra. Iron spectra recorded by XEUS were already studied before,⁹ while copper spectra have not yet been employed in NSTX plasma impurity diagnostics. The x-ray spectrum presented in Fig. 1 (top) was accumulated over three NSTX shots (134191, 134192, and 134195). During these shots the maximum electron temperature was between 1.1 and 1.25 keV and maximum electron densities varied from 7×10^{13} to 9×10^{13} cm $^{-3}$. This spectrum covers a spectral range from 8 to 18 Å which includes L-shell Cu spectrum between 8 and 13.5 Å shown in more detail in Fig. 2. The spectral resolution ($\lambda/\Delta\lambda$) of about 100 was enough to resolve the most intense Ne-like Cu lines as well as less intense F- and O-like Cu spectra features but not sufficient to resolve the Na-like peaks Na1 and Na2 (located between Ne-like 3C and 3D lines). The theoretical fit is good except for the most intense Ne-like 3-2 lines, 3C, 3F, and 3G because of the following reasons. This spectrum is a spatially

and time-integrated spectrum and it is well known that Ne-like ions dominate the ionization balance over a wide range of electron temperatures. Then, it is possible that Ne-like Cu spectra represent a superposition from different plasma regions and could not be described by a one-temperature model. The spectra from higher ionization stages came from higher-temperature regions with more similar temperatures. The additional distinct features of the L-shell Cu spectrum are the somewhat higher intensity of the N-like peak and the appearance of the C-like peak, which results, for example, in a higher fraction of N-like Cu ions (0.19). The identification of the above mentioned different ionization states allows for estimates of the charge state distribution (CSD). Charge balance coefficients were derived from the most intense peak for each respective ion using the fit of the experimental spectrum. The estimated CSD gives an average ion charge $\langle Z \rangle = 20.26$. The spectral region between 12 and 12.5 Å is the most complex and challenging for identification because it includes the contribution from Cu, Fe, and Ni ions. In particular, the line at 12.429 Å was assigned to the Ne-like 3C Ni line (see Fig. 2, top). The longer wavelength spectral region above 13.5 Å is dominated by L-shell Fe lines and K-shell O lines (H-like lines due to transitions $np \rightarrow 1s$ for $n=3, 4, \text{ and } 5$, i.e., $Ly\beta$, $Ly\gamma$, and $Ly\delta$, respectively). The comparatively strong O-like Fe spectral feature around 13.5 Å indicates an electron temperature higher than that derived from L-shell Cu spectrum, while in general the Ne-like Fe spectrum is much less intense than Ne-like Cu spectrum.

IV. ANALYSIS OF Z-PINCH Cu PLANAR WIRE ARRAY SPECTRUM

The Z-pinch experiment was performed on the 1 MA Zebra generator at UNR. The wire array load was a planar wire array (PWA) with 12 10 μm Cu wires arranged in a single planar row with an interwire gap of 0.7 mm. The distance between the anode and cathode (length of the wires) was 20 mm. Time-integrated spatially resolved spectra of implosions of the PWA were recorded by a convex spectrometer with a potassium hydrogen phthalate (KAP) crystal with a radius of curvature of 50.8 mm, a special resolution of 0.5 mm, and a spectral resolution ($\lambda/\Delta\lambda$) of 300. They cover the spectral region from 7 to 14 Å, which includes L-shell Cu spectrum. The example of such an experimental spectrum (x-ray image and lineout positioned near the anode) is presented in Fig. 3 together with the synthetic spectra. The L-shell Cu modeling in the optically thin approximation produced a good fit of this spectrum except for the intensity of the 3C line (which is reduced in the experiment by opacity). Not only the most intense Ne-like lines but also the spectral features from higher ionization states such as F- and O-like Cu ions are clearly seen. From modeling, it follows that the presence of the strong 3F and 3G lines indicate an electron density not higher than 10^{18} cm^{-3} , while the prominent F-like and particular O-like spectral features indicate electron temperatures higher than 400 eV. Many spectral features from different ions are blended together so that the spectral resolution is an important factor for the correct identification

and theoretical fit. For example, the diagnostically important Ne-like 3A line is strongly blended with the O2 peak. The spectral resolution of 300 determined in this experiment was enough to resolve all ionization states that contribute to the spectrum, from Na-like to Ne-like to N-like Cu ions, and to make estimates of the CSD.

The Ne-like Cu spectrum was fit to the 3F and 3G lines, and the fit was verified with the 4C and 4D lines. The F-like Cu spectrum was fit with the F1 spectral features and verified with the less intense F4 spectral peak. The O- and the N-like Cu spectra were fit to the O1 and N1 peaks, respectively, and the Na-like Cu spectrum was fit to the Na2 peak. As a result, the estimated CSD was found to be 0.33 for Ne-like, 0.27 for F-like, 0.19 for O-like, 0.11 for Na-like, and 0.1 for N-like Cu ions, and the average ion charge $\langle Z \rangle = 19.84$.

V. CONCLUSION

In conclusion, a detailed study of x-ray spectra in the range 7–18 Å, which includes not only the well known and commonly seen iron spectra but also copper spectra was accomplished. The L-shell copper spectra have not yet been employed as an NSTX plasma impurity diagnostic and the present analysis is the first to perform a detailed modeling of the Cu L-shell emission from NSTX. In particular, the L-shell Cu spectra were modeled and predictions were made for identifying contributions from various Cu ions in different spectral bands along with L-shell spectral features from Fe ions and some Ni ions. Also, similar spectra but from much denser Cu plasmas produced on the UNR Z-pinch facility were analyzed and compared with the NSTX data.

ACKNOWLEDGMENTS

This work was supported by the DOE under Grant No. DE-FG02-08ER54951 and in part under the NNSA Cooperative Agreement Nos. DE-FC52-06NA27588 and DE-FC52-06NA27586. Work at the LLNL was performed under auspices of the DOE under Contract No. DE-AC52-07NA2344.

¹B. C. Stratton, M. Bitter, K. W. Hill, D. L. Hillis, and J. T. Hogan, *Fusion Sci. Technol.* **53**, 431 (2008).

²P. Beiersdorfer, M. Bitter, L. Roquemore, J. K. Lepson, and M. F. Gu, *Rev. Sci. Instrum.* **77**, 10F306 (2006).

³P. Beiersdorfer, J. K. Lepson, M. Bitter, K. W. Hill, and L. Roquemore, *Rev. Sci. Instrum.* **79**, 10E318 (2008).

⁴J. K. Lepson, P. Beiersdorfer, J. Clementson, M. F. Gu, M. Bitter, L. Roquemore, R. Kaita, P. G. Cox, and A. S. Safronova, *J. Phys. B* **43**, 144018 (2010).

⁵A. S. Safronova, V. L. Kantsyrev, A. A. Esaulov, N. D. Ouart, M. F. Yilmaz, K. M. Williamson, V. Shlyaptseva, I. Shrestha, G. C. Osborne, C. A. Coverdale, B. Jones, and C. Deeney, *Rev. Sci. Instrum.* **79**, 10E315 (2008).

⁶M. F. Gu, *Can. J. Phys.* **86**, 675 (2008).

⁷A. S. Safronova, V. L. Kantsyrev, N. Ouart, F. Yilmaz, D. Fedin, A. Astanovitsky, B. LeGalloudec, S. Batie, D. Brown, V. Nalajala, S. Pokala, I. Shrestha, T. E. Cowan, B. Jones, C. A. Coverdale, C. Deeney, S. B. Hansen, P. D. LePell, D. Jobe, and D. Nielson, *J. Quant. Spectrosc. Radiat. Transf.* **99**, 560 (2006).

⁸C. A. Coverdale, A. S. Safronova, V. L. Kantsyrev, N. D. Ouart, A. A. Esaulov, C. Deeney, K. M. Williamson, G. C. Osborne, I. Shrestha, D. J. Ampleford, and B. Jones, *Phys. Rev. Lett.* **102**, 155006 (2009).

⁹P. Beiersdorfer, E. Magee, E. Träbert, H. Chen, J. K. Lepson, M. F. Gu, and M. Schmidt, *Rev. Sci. Instrum.* **75**, 3723 (2004).